

## Research Article

# Highly Dispersed Pt-Sn/GNS Catalysts for Ethanol Electro-Oxidation in Membraneless Fuel cells

S. Thilaga<sup>1</sup>, V. Selvarani<sup>1</sup>, S. Durga<sup>1</sup>, S. Kiruthika<sup>2</sup>, B. Muthukumar<sup>1,\*</sup>

<sup>1</sup>Department of Chemistry, Presidency College, Chennai – 600 005, India.

<sup>2</sup>Department of Chemical Engineering, SRM University, Chennai – 603 203, India.

\*Corresponding author's e-mail: [dr.muthukumar@yahoo.com](mailto:dr.muthukumar@yahoo.com)

## Abstract

In the present work, Pt–Sn catalysts were synthesized on graphene nanosheets and their electrocatalytic activity for ethanol oxidation in membraneless fuel cell was investigated and compared with Vulcan XC-72R carbon supports. The physicochemical characterizations demonstrated that all the catalysts have the Pt face-centered cubic (fcc) structure with variations in the lattice parameter, indicating the incorporation of Sn after alloying. In comparison to carbon supports, the mean particle sizes of graphene-supported Pt–Sn catalysts were smaller. The electrochemical results obtained at room temperature showed that the Pt–Sn catalysts supported on graphene nanosheets showed superior electrochemical activity toward ethanol oxidation compared to Pt–Sn/Vulcan XC-72R. The enhancement of the electrocatalytic activities were discussed with respect to Pt–Sn alloy formation and the resulting modification of the electronic properties of Pt by Sn in the alloy structure. During the experiments performed on single membraneless fuel cells, graphene-supported Pt–Sn catalysts performed better than the carbon supported catalysts with power density of  $37.5 \text{ mW cm}^{-2}$ . The better performance of graphene-supported catalysts may be due to the significant increase of electrochemical active surface area and the smaller particle size.

**Keywords:** Ultrasonic-assisted chemical reduction; Graphene nanosheets; Sodium percarbonate; Membraneless fuel cells.

## Introduction

Fuel cells are considered to be alternatives to our present power sources because of their high operational efficiencies and environment-friendly working characteristics [1]. The best and standard catalyst routinely used in fuel cells is Pt/C [2], However, Pure platinum is poisoned by strongly adsorbed species like CO, which is generated from the dissociation of organic molecules and thus the reactivity of platinum reduces [3]. Several platinum based alloy such as Pt-W [4], Pt-Sn [4], Pt-Ru [5], Pt-Rh [6] have been proposed to address these problem. Among these alloys, bimetallic Pt–Sn catalysts have been demonstrated a superior activity toward electrooxidation of ethanol and these catalysts diminished the poisoning effect of CO because the OH groups that are generated on Sn promote the oxidation of CO on the Pt catalyst. Thus, Sn plays an important role in the ethanol electrooxidation and consequently improves fuel cell performance [7].

In addition to the various types of alloy materials and composition ratios, the choice of a suitable catalyst support material is also important. Carbon materials such as activated carbons [8], graphite nanofibers (GNF) [9], and carbon nanotubes (CNT) [10] have been studied as catalyst support materials. Among them, CNTs have been paid more attention to in fuel cells because of their extraordinary electronic and catalytic properties. It is well known that metal particles on CNTs show outstanding properties and improved catalytic activity [11]. In comparison with CNTs, graphene nanosheets (GNS) not only possess similar stable physical properties, but also large surface areas (theoretical specific area of  $\sim 2630 \text{ m}^2 \text{ g}^{-1}$ ) that can be considered as plat CNTs. In addition, the production cost of GNS on a mass scale is cheaper than that of CNTs [12]. Also, GNS have been reported to have good dispersion stability and large surface areas [13,14].

In this study we report on the preparation of Pt-Sn electrocatalysts supported on graphene nanosheets (GNSs) as well as Vulcan XC-72R carbon (C) using the ultrasonic-assisted chemical reduction method in which ethylene glycol (EG) is used as solvent and reducing agent at the same time. The electrocatalytic activity of the prepared catalysts toward ethanol electrooxidation in membraneless ethanol fuel cell (MLEFC) has been evaluated and discussed in relation to the structural properties and compared with the Vulcan XC-72R carbon black catalyst supports.

## Materials and methods

### Chemicals and materials

The metal precursors used for the preparation of electrocatalysts were  $\text{H}_2\text{PtCl}_6 \cdot 6\text{H}_2\text{O}$  (from Aldrich), and  $\text{SnCl}_2 \cdot 2\text{H}_2\text{O}$  (from Alfa Aesar). Graphene oxide (from Sigma-Aldrich), and Vulcan Carbon XC-72R (from Cabot Corp.) was used as a support for the catalysts. Ethylene glycol (from Merck) was used as the solvent and reduction agent. Nafion<sup>®</sup> (DE 521, DuPont USA) dispersion was used to make the catalyst ink. Ethanol (from Merck), sodium percarbonate (from Riedel) and  $\text{H}_2\text{SO}_4$  (from Merck) were used as the fuel, the oxidant and as the electrolyte for electrochemical analysis, respectively. All the chemicals were of analytical grade. Pt/C (40-wt%, from E-TEK) was used as the cathode catalyst.

### Catalyst preparation

GNS was prepared by modified Hummer's chemical oxidation method. First, chemical oxidation in  $\text{H}_2\text{SO}_4$  and  $\text{H}_2\text{O}_2$  causes greater interlayer distance of graphite and oxidized graphite sheet is exfoliated by ultrasonication for 3 h. Then, highly loaded Pt-Sn/GNS catalyst was synthesized by ultrasonic-assisted chemical reduction according to the following procedures. 100 mg of GNS powder was dispersed in 30 ml of ethylene glycol (EG) solution and sonicated for 1 h. Subsequently, 2 ml of hexachloroplatinic acid-EG ( $\text{H}_2\text{PtCl}_6$ -EG) solution (6.25 mg/mL) and 2 ml of tin dichloride-EG ( $\text{SnCl}_2$ -EG) solution (4.47 mg/ml) were added to this dispersion and sonicated for 2 h. The pH of the solution was adjusted to 10 using sodium hydroxide-EG (NaOH-EG) solution (0.5 mol/L), and then the solution was stirred under flowing argon at 120 °C for 3 h. The solid material produced was then centrifuged, washed

3 times with deionized water and finally dried in a vacuum oven at 80 °C for 24 h. Similar procedures were used to prepare carbon black (Vulcan XC-72R) supported-Pt-Sn (Pt-Sn/C) catalysts. The nominal loading of metals in the electrocatalysts was 40 wt.%.

### Structural catalyst characterization

The morphology of the dispersed catalysts was examined using TEM (Philips CM 12 Transmission Electron Microscope). The particle size distribution and mean particle size were also evaluated using TEM. The crystal structure of the synthesized electrocatalysts was characterized by powder X-ray diffraction (XRD) using a Rigaku multiflex diffractometer (model RU-200 B) with  $\text{Cu-K}\alpha_1$  radiation source ( $\lambda_{\text{K}\alpha_1} = 1.5406 \text{ \AA}$ ) operating at room temperature. The tube current was 40 mA with a tube voltage of 40 kV. The  $2\theta$  angular regions between 20° and 90° were recorded at a scan rate of 5°  $\text{min}^{-1}$ . The mean particle size analyzed from TEM is verified by determining the crystallite size from XRD pattern using Scherrer formula [14]. Pt (2 2 0) diffraction peak was selected to calculate crystallite size and lattice parameter of platinum. The atomic ratio of the catalysts was determined by an energy dispersive X-ray (EDX) analyzer, which was integrated with the TEM instrument.

### Electrochemical measurements and electrode preparation

All electrochemical measurements were carried out using an electrochemical workstation (CHI-6650; CH Instruments, USA) in a conventional three electrode cell assembly consisting of the glassy carbon disk as a working electrode, Pt foil as a counter electrode and Ag/AgCl as a reference electrode. The working glassy carbon electrode was prepared by the following steps: first, 10 mg of Pt-Sn/GNS catalyst was suspended in a mixed solvent (isopropyl alcohol (500  $\mu\text{L}$ ), water (500  $\mu\text{L}$ ) and 5 wt.% Nafion solution (100  $\mu\text{L}$ , Aldrich)) with ultrasonication for 20 min. 10  $\mu\text{L}$  of ultrasonically homogenized ink was drop-coated onto a freshly polished glassy-carbon electrode ( $A = 0.125 \text{ cm}^2$ ) and the solvent was then evaporated in open air at room temperature. A similar procedure was used for the Pt-Sn/C catalyst. The loading of metal on the working electrode was  $0.28 \text{ mg}_{\text{metal}} \text{ cm}^{-2}$ . The

electrochemical activity of the ethanol oxidation reaction was measured by cyclic voltammetry in a half cell at a scan rate of  $50 \text{ mV s}^{-1}$  at room temperature in a 1 M  $\text{CH}_3\text{CH}_2\text{OH}$  and 1 M  $\text{H}_2\text{SO}_4$  solution. All potentials in this paper were scaled versus Ag/AgCl.

## Results and discussions

### Structural characterization

#### X-ray diffraction (XRD)

XRD analyses were performed to obtain structural information of the catalyst and its support. Fig. 1 shows the XRD patterns of Pt-Sn/GNS as well as Pt-Sn/C catalysts. The peak at  $27^\circ$  is associated with the (0 0 2) plane of graphene, revealing the successful reduction of the graphite oxide to graphene. The strong diffraction peak at  $2\theta$  of  $\sim 40^\circ$  and other three peaks at  $\sim 46^\circ$ ,  $67^\circ$ , and  $81^\circ$  are attributed to the Pt (1 1 1), (2 0 0), (2 2 0), and (3 1 1) crystalline planes, respectively, which represents the typical character of crystalline Pt with face-centered cubic (FCC) crystalline structure [16,17]. Relative to pure Pt, the diffraction peaks are shifted to lower  $2\theta$  values than the reference

vertical line of Pt, which suggests that a Pt-Sn alloy is formed. This shift can be explained by the enlargement of lattice constant which is caused by Sn incorporation. The peaks of the  $\text{SnO}_2$  phase at  $34^\circ$  and  $52^\circ$  were clearly observed for Pt-Sn/C catalyst, while for Pt-Sn/GNS only the peaks characteristic of the Pt fcc structure were observed, but their presence cannot be discarded because they may be present in a very small particle size. The lattice parameters and the average crystallite size of the catalysts obtained from the XRD patterns are listed under Table 1.

The fcc lattice parameters were evaluated from the angular position of the (2 2 0) peaks and the calculated value for Pt-Sn/GNS (0.3994 nm) were larger than that of Pt-Sn/C catalysts (0.3987 nm), indicating a lattice expansion caused by the incorporation of Sn into the fcc structure of platinum after alloying. The average crystallite size was estimated using the Scherrer equation. The lattice parameters and the average crystallite size of the catalysts obtained from the XRD patterns are listed in Table 1.

Table 1. Characterization parameters for the Pt-Sn/C and Pt-Sn/GNS nanocatalysts

Electrocatalysts		(220) Diffraction peak position ( $2\theta^\circ$ )	Lattice parameter (nm)	Average crystallite size from XRD (nm)	Average Particle size from TEM (nm)
Nominal	Experimental				
Pt <sub>50</sub> Sn <sub>50</sub> /C	Pt <sub>52</sub> Sn <sub>48</sub> /GNS	66.24	0.3987	3.8	3.2
Pt <sub>50</sub> Sn <sub>50</sub> /GNS	Pt <sub>49</sub> Sn <sub>51</sub> /C	66.10	0.3994	3.6	2.7

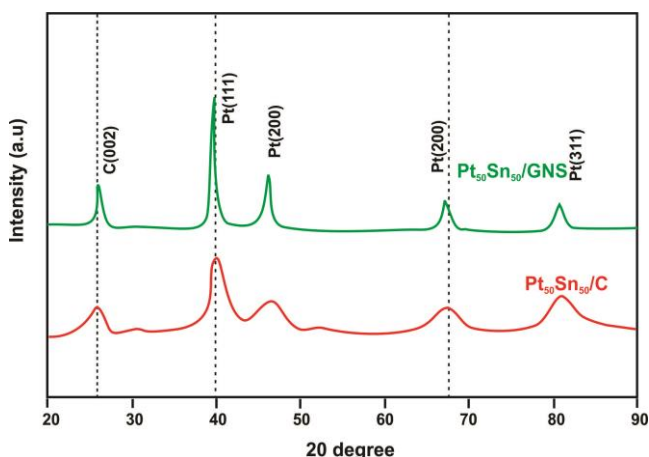


Fig. 1. X-ray diffraction patterns of Pt-Sn/GNS and Pt-Sn/C

#### Transmission electron microscopy (TEM)

The TEM images of Pt-Sn/GNS as well as Pt-Sn/C catalysts are shown in Fig. 2. The Pt-Sn particles are successively dispersed on both specimens. However, comparing with Pt-Sn/C, the small black Pt-Sn/GNS particles are more uniformly dispersed on the graphene sheets than on the carbon supports. It can be seen from the images that the metal particle sizes of each sample are less than 4 nm, and they are of spherical shape. In comparison to Pt-Sn/C the mean particle size of Pt-Sn/GNS were smaller. This particle dispersion and size difference can be explained by the different specific surface areas of carbon support materials. The particle size distribution of these catalysts is shown in

Table 1 in accordance to the TEM images. The mean particle size found by TEM image and

XRD analysis were similar.

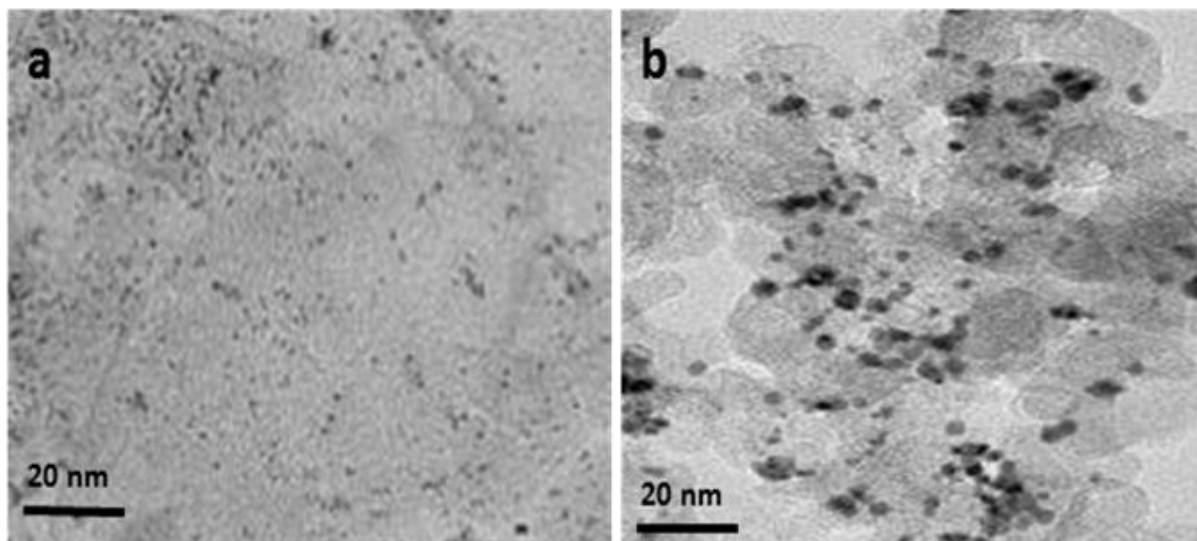


Fig. 2. TEM images of a) Pt-Sn/GNS, b) Pt-Sn/C catalysts

#### Energy dispersive X-ray (EDX) analysis

The EDX analyses of Pt-Sn/GNS as well as Pt-Sn/C, catalysts are shown in Fig. 3. The EDX results are shown in Table 1. The results of EDX analysis proves that the particles are very close to the nominal values of Pt and Sn. We have found from EDX result that the Pt:Sn atomic ratio are closely 1:1, which is conceded to be the most active composition for the ethanol electro-oxidation reaction [19].

#### Electrochemical characterization

##### Cyclic voltammetry (CV)

Fig. 4 shows the cyclic voltammetry of Pt-Sn/GNS as well as Pt-Sn/C electrocatalysts deposited onto glassy-carbon electrode in the absence of ethanol. Typical hydrogen adsorption/desorption peaks are observed in the potential range  $-0.2$  to  $0.1$  V (vs. Ag/AgCl). The hydrogen adsorption of Pt-Sn/GNS is apparently larger than those of Pt-Sn/C, suggesting that may be due to the smaller particle size of the catalysts. The intensity of the peak current normalized by the weight of Pt in catalyst revealed the electrochemical activity of ethanol oxidation.

It is well-known that the electrochemically active surface area (ECSA) reveals the available number of active sites on the catalyst surface for electrochemical reactions and determines the efficient transport routes for electrons on the electrode surface; therefore, the larger the ECSA, the higher the electrocatalytic activity for

ethanol oxidation. The ECSA of different catalysts can be calculated according to Eq. (2) [20].

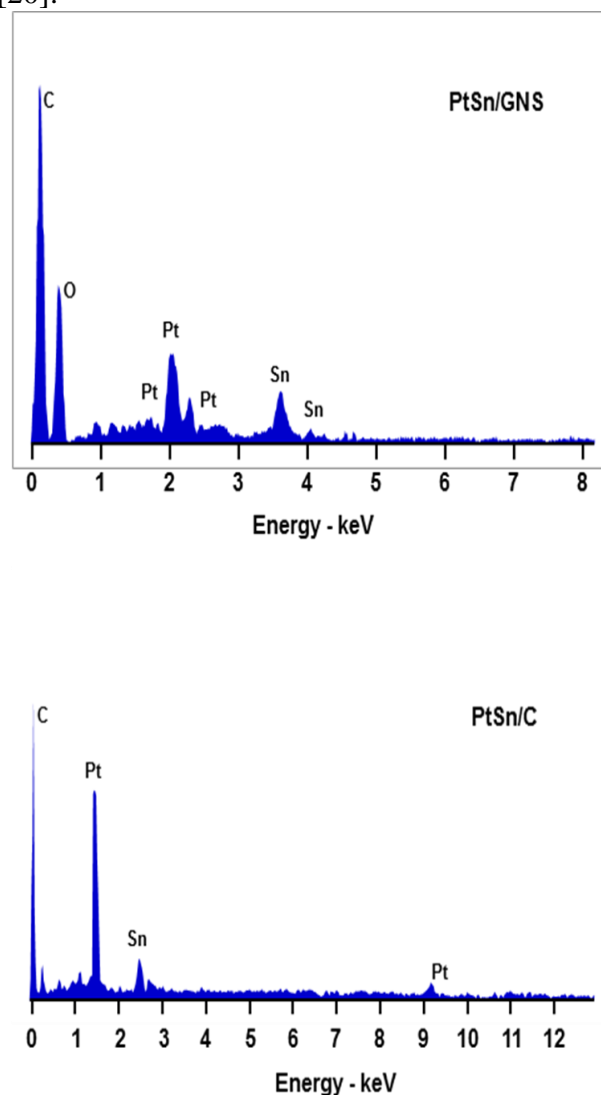


Fig. 3. EDX spectra of a) Pt-Sn/GNS, b) Pt-Sn/C catalysts

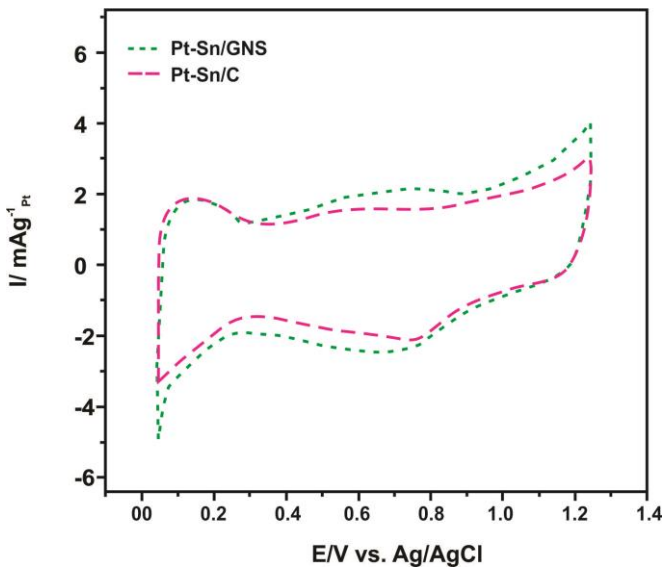


Fig. 4. Cyclic voltammetry of Pt–Sn/GNS and Pt–Sn/C nanocatalysts in 0.5 M H<sub>2</sub>SO<sub>4</sub> at room temperature with a scan rate of 50 mV s<sup>-1</sup>

$$S_{ECSA/H} (m^2/g) = \frac{Q_H (\mu C/cm^2)}{210 (\mu C/cm^2) \times 0.77 \times [Pt]} \quad (1)$$

$$S_{ECSA/CO} (m^2/g) = \frac{Q_{CO} (\mu C/cm^2)}{420 (\mu C/cm^2) \times [Pt]} \quad (2)$$

Where  $Q_H$  is the charges corresponding to desorption of hydrogen on the Pt surface, [Pt] (mg/cm<sup>2</sup>) is the Pt loading on the electrode surface, 210 μC/cm<sup>2</sup> is the charge required to oxidize a monolayer of hydrogen on the Pt surface, and 0.77 is the hydrogen monolayer

Table 2. Comparison of the hydrogen desorption charge, the carbon monoxide desorption charge, and its electrochemical active surface area and electrode roughness

Catalyst	$Q_H/\mu C$	$Q_{CO}/\mu C$	Electrode real surface area (cm <sup>2</sup> )	$ECSA/CO (m^2 g_{Pt}^{-1})^a$	Roughness
Pt-Sn/C	293	762	1.81	36.3	50.82
Pt-Sn/GNS	354	919	2.19	43.8	61.32

<sup>a</sup>The electrochemical active surface areas ( $S_{ECSA/H}$  and  $S_{ECSA/CO}$ ) were calculated from Eq. (1) and Eq.(2).

Table 3. CV results of Pt-Sn/C and Pt–Sn/GNS nanocatalysts at room temperature

Catalysts	Forward	Backward	$I_F/I_R$ ratio
	anodic peak ( $I_F$ ) (mA cm <sup>-2</sup> )	anodic peak ( $I_R$ ) (mA cm <sup>-2</sup> )	
Pt-Sn/C	30.2	19.2	1.5
Pt-Sn/GNS	43.7	24.2	1.8

The nanocatalysts in our work, the Pt–Sn/GNS catalysts exhibited a higher  $I_F/I_R$  value (1.8) than the Pt–Sn/C (1.5), indicating the much more complete oxidation of ethanol in the

coverage [43]. The ECSA of different catalysts were calculated based on Eq. (2) and are listed in Table 2. The calculated ECSA of Pt–Sn/GNS (43.8 m<sup>2</sup>/g<sub>Pt</sub><sup>-1</sup>), were higher than that of Pt–Sn/C (36.3 m<sup>2</sup>/g<sub>Pt</sub><sup>-1</sup>). It indicated that the smaller particle size and better dispersion of catalysts on the graphene nanosheets has a significant impact on improving the ECSA value.

Fig. 5 shows the cyclic voltammograms (CV) of ethanol electro-oxidation catalyzed by Pt–Sn/GNS as well as Pt–Sn/C catalysts in a 1.0 M C<sub>2</sub>H<sub>5</sub>OH and 0.5 M H<sub>2</sub>SO<sub>4</sub> solution at room temperature. In graphene nanosheets as well as Vulcan XC-72R carbon supported Pt–Sn electrodes, two oxidation current peaks can be observed on the forward and backward scan due to EOR. The peak in the forward scan is associated with the ethanol oxidation, and the peak in the reverse scan is related to the oxidation of carbonaceous intermediate products formed from incomplete ethanol oxidation.

The ratio of the forward peak current ( $I_F$ ) to the reverse peak current ( $I_R$ ) can be used to evaluate the tolerance of the catalysts to the accumulation of the intermediate carbonaceous species [13]. A higher  $I_F/I_R$  value indicates higher tolerance of intermediate carbon species. The data obtained from Fig. 5 are also listed in Table 3.

forward scan and the effective removal of poisoning CO-like species from the surface of catalysts. As shown in Fig. 5, the onset potentials of Pt–Sn/GNS for ethanol electro-oxidation were

noted at 0.25 V, while the onset potentials on Pt-Sn/C were at 0.30 V vs. Ag/AgCl respectively. In addition, the results not only indicate that the peak potentials shift to negative direction on Pt-Sn/GNS compared with Pt-Sn/C, but also reveal that the peak current densities become much larger, indicating ethanol electro-oxidation is

more active on GNS based catalysts than that on carbon supported catalysts. Table 4 summarizes the CV results of the prepared electrocatalysts including the onset potentials, positive peak potentials and the corresponding peak current densities of EOR.

Table 4. Positive peak potential and Peak current density of Pt/C, Pt-Sn/C and Pt-Sn/GN nanocatalysts at room temperature

Catalyst	Onset potential (V)	Scan rate 50 mVs <sup>-1</sup>	
		Positive peak potential (V vs. Ag/AgCl)	Peak current density (mA cm <sup>-2</sup> )
Pt-Sn/C	0.30	0.77	30.2
Pt-Sn/GNS	0.25	0.75	43.7

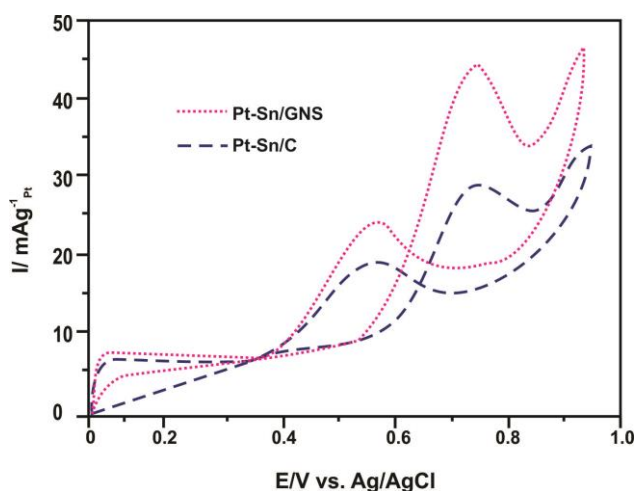


Fig. 5. Cyclic voltammetry of Pt-Sn/GNS and Pt-Sn/C nanocatalysts in 0.5 M H<sub>2</sub>SO<sub>4</sub> and 1.0 M Ethanol at room temperature with a scan rate of 50 mVs<sup>-1</sup>

#### Chronoamperometry (CA)

The Pt-Sn/GNS, Pt-Sn/C electrocatalyst performances for ethanol oxidation were studied by chronoamperometry at 0.4V for two hours, to evaluate both the electrocatalytic activity of the catalysts and the poisoning of the active surface under continuous operation conditions. Fig. 6 shows representative chronoamperograms obtained for the different electrocatalysts whose current densities were normalized by Pt mass.

During the first few minutes, there was a sharp decrease in the current density and after some time, it becomes relatively stable. This behavior can be explained assuming that initially the active sites are free from adsorbed ethanol molecules, but a new adsorption of ethanol molecules is a function of the liberation of the

active sites by ethanol oxidation and intermediate species (CO, CH<sub>x</sub>, CH<sub>3</sub>CHO and CH<sub>3</sub>COOH) formed during the first minutes, which are responsible for poisoning of the catalytic sites [11].

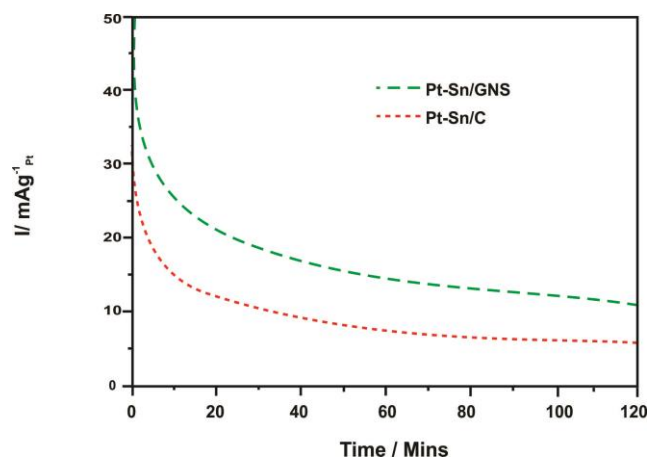


Fig. 6. Chronoamperometry of Pt-Sn/GNS and Pt-Sn/C nanocatalysts in 0.5 M H<sub>2</sub>SO<sub>4</sub> at room temperature with a scan rate of 50 mV s<sup>-1</sup>

The Graphene supported Pt-Sn electrocatalysts gave higher current than the carbon supported Pt-Sn electro-catalysts. This may indicate that the high surface area and high conductivity, making the graphene supported electrocatalysts better candidates for ethanol electro-oxidation than carbon supported electrocatalysts. Furthermore, the addition of Sn to Pt/GNS and Pt/C could reduce the CO poisoning and enhance the activity and stability of Pt nanoparticles on ethanol through its oxygen-containing species. Similar results were observed by Karim [21] for ethanol oxidation by using catalysts prepared by Ethylene glycol reduction process.

Single cell performance

The, PtSn/GNS, PtSn/C, catalysts were evaluated as anode catalysts for ethanol electro-oxidation by single membraneless ethanol fuel cell. When Pt/C (100) was used as the anode catalyst, the performance of membraneless ethanol fuel cell was found to be poor. The results of MLEFC adapting to different catalysts are summarized in Table 5. When the current was normalized to the geometric area of single cell, it was observed that the cell performance of graphene supported Pt-Sn catalyst was better than that of other catalysts. The OCP for Pt-Sn/GNS catalyst was 0.81 V higher than that of

Pt-Sn/C (0.68 V) catalyst respectively. In addition there was a rapid initial fall in cell voltage for all catalysts, which was due to the slow initial ethanol electro-oxidation reaction at the electrode surface. After a initial drop of 50 mV the change in the slope of the polarization curve for Pt-Sn/GNS decreased, and it started drawing more current. This event can be attributed to the more effective catalytic ability of Pt-Sn/GNS, once the EOR reaction is initiated. Based on the peak power density drawn from a single cell, Pt-Sn/GNS is the best anode catalyst with a peak power density value of 37.5mW/cm<sup>2</sup>.

Table 5. Summary of the performance of single fuel cell tests using Pt-Sn/C and Pt-Sn/GNS nanocatalysts

Anode Catalysts	Open circuit voltage (V)	Maximum Power density (mW cm <sup>-2</sup> )	Maximum Current density (mA cm <sup>-2</sup> )
Pt-Sn/C	0.68	25.8	150
Pt-Sn/GNS	0.81	37.5	213

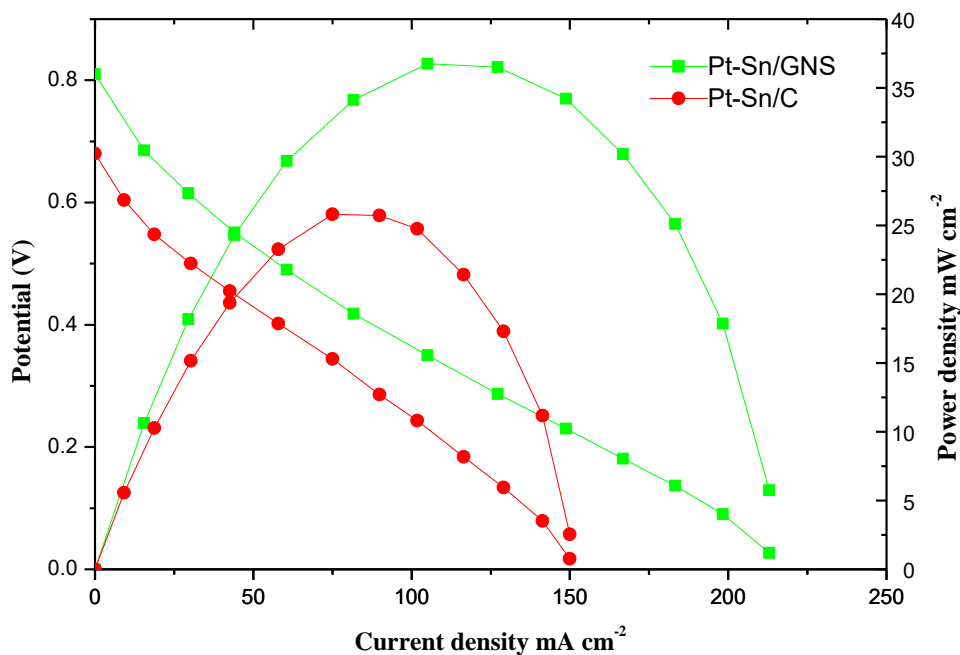


Fig. 7. Polarization and power density curves of Pt-Sn/GNS and Pt-Sn/C nanocatalysts

Figure 7 shows the polarization curves of the membraneless ethanol fuel cell at room temperature. The peak power density and current density were about (37.5 mW/cm<sup>2</sup> and 213 mA/cm<sup>2</sup>) for the graphene supported Pt-Sn catalyst, which are much higher than those of the carbon supported Pt-Sn (25.8 mW/cm<sup>2</sup> and 150 mA/cm<sup>2</sup>) catalysts. Both the large power density

and current density should be attributed to the excellent catalytic activity of Pt-Sn/GNS for ethanol oxidation. The results indicate that compared to Vulcan carbon more surface available on graphene nanosheet for electrochemical reaction and better mass transport in the catalyst layer.

## Conclusions

Graphene nanosheet (GNS) and carbon supported Pt-Sn nanocatalyst for ethanol oxidation is presented in this study. Graphene nanosheets were synthesized by the modified Hummer's method by loading 40 wt.% Pt and Pt-Sn nanoparticles on to a graphene nanosheet, using an improved ultrasonic-assisted chemical reduction method. The synthesis results show that the Pt-Sn nanoparticles are uniformly dispersed on the graphene nanosheets compared to the Vulcan XC-72R carbon. In comparison to Vulcan XC-72R carbon as a catalyst support, graphene nanosheets can more effectively enhance the electrocatalytic activity of Pt-Sn nanoparticles for the oxidation of ethanol into CO<sub>2</sub>, which is attributed to the special structure of the graphene nanosheets. These qualities achieve a considerably higher ECSA value and a larger catalytic current density for ethanol oxidation, as well as a far higher  $I_F/I_R$  value, for GNS-supported catalysts compared to the Vulcan XC-72R carbon. Considering its facile process and superior performance for ethanol oxidation, GNS is a promising support material for electrocatalysts.

## Acknowledgments

The financial support for this research from the University Grants Commission (UGC), New Delhi, India, through a Major Research Project 42-325/20134 (SR) is gratefully acknowledged.

## Conflict of interest

Authors declare there are no conflicts of interest.

## References

- [1] Kundu A, Jang J, Gill J, Jung C, Lee H, Kim S, Ku B, Oh Y. Micro-fuel cells-Current development and applications. *J Power Sources*. 2007;170:67-78.
- [2] Morse JD. Micro fuel cell power source. *Int J Energy Res*. 2007;31:576-602.
- [3] Tsang CW, Harrison AG. Chemical ionization of amino acids. *J Am Chem Soc*. 1976;98:1301-1308.
- [4] Teresa I, Elena P. FTIR spectroscopic investigation of adsorbed ethanol on polycrystalline platinum. *Electrochimica Acta*. 1994;39:531-537.
- [5] Li YS, Zhao TS. Understanding the performance degradation of anion-exchange membrane direct ethanol fuel cells. *Int J Hydrogen Energy*. 2012;37:4413-4421
- [6] Zignani C, Gonzalez ER, Baglio V, Siracusano S, Arico AS. Investigation of a Pt<sub>3</sub>Sn/C electro-catalyst in a direct ethanol fuel cell operating at low temperature for portable applications. *Int J Electrochem Sci*. 2012;7:3155-3166.
- [7] Antolini E. Catalysts for direct ethanol fuel cells. *J Power Sources*. 2007;170:1-12.
- [8] Dattta J, Singh S, Das S, Bandyopadhyay NR. A comprehensive study on the effect of Ru addition to Pt electrodes for direct ethanol fuel cell. *Bulletin of Material Science*. 2009;32:643-652.
- [9] Abu B, Ahmed AN, Illya S, Marga-Martina P, Wolfgang G, Michael B. Rapid microwave-assisted polyol reduction for the preparation of highly active PtNi/CNT electrocatalysts for methanol oxidation. *ACS Catal*. 2014;4(8):2449-2462.
- [10] Ramos SG, Calafiore A, Bonesi AR, Triaca WE, Castro Luna AM, Moreno MS, Zampieri G, Bengio S. Supported catalysts for alcohol oxidation synthesis and analysis of their catalytic activity. *Int J Hydrogen Energy*. 2012;32:995-1001.
- [11] Cunha EM, Ribeiro J, Kokoh KB, de Andrade AR. Preparation, characterization and application of Pt-Ru-Sn/C trimetallic electrocatalysts for ethanol oxidation in direct fuel cell. *Int J Hydrogen Energy*. 2011;3:11034-11042.
- [12] Almeida TS, Kokoh KB, De Andrade AR. Effect of Ni on Pt/C and PtSn/C prepared by the pechini method. *Int J Hydrogen Energy*. 2011;36:3808-3810.
- [13] Yong W, Xiaomin W, Yongzhen W, Jinping L. Acid-treatment-assisted synthesis of Pt-Sn/graphene catalysts and their enhanced ethanol electro-catalytic activity. *Int J Hydrogen Energy*. 2015;40:990-997.
- [14] Radmilovic V, Gasteiger HA, Ross Jr. PN. Structure and chemical composition of a supported Pt-Ru electrocatalyst for methanol oxidation. *J Catal*. 1995;154:98-106.
- [15] Fei H, Xiaomin W, Jie L, Yongzhen W. The effect of Sn content on the electrocatalytic properties of Pt-Sn nanoparticles dispersed on graphene nanosheets for methanol oxidation



- oxidation reaction. *Carbon*. 2012;50:5498-5504.
- [16] Borgna A, Stagg SM, Resasco DE. Interference phenomena in the EXAFS spectra of Pt-Sn bimetallic catalysts. *J Phys Chem B*. 1998;102:5077-5081.
- [17] Zhou ZH, Wang SL, Zhou WJ, Jiang LH, Wang GX, Sun GQ, Zhou B, Xin Q. . Preparation of highly active Pt/C cathode electrocatalysts for DMFCs by an improved aqueous impregnation method. *Phys Chem Chem Phys*. 2003;5:5485-5488.
- [18] Ponmani K, Nayeemunisha SM, Kiruthika S, Muthukumaran B. Electrochemical characterization of platinum based anode catalysts for membraneless fuel cells. *Ionics*. 2015;19:1-11.
- [19] Arun A, Gowdhamamoorthi M, Ponmani K, Kiruthika S, Muthukumaran B. Electrochemical characterization of Pt-Ru-Ni/C anode electrocatalyst for methanol electrooxidation in membraneless fuel cell. *RSC Adv*. 2015;5:49643-49650.
- [20] Li Y, Gao W, Ci L, Wang C, Ajayan PM. Catalytic performance of Pt nanoparticles on reduced graphene oxide for methanol electro-oxidation. *Carbon*. 2010;48:1124-1130.
- [21] Karim K. Decoration of graphene oxide with Platinum Tin nanoparticles for ethanol oxidation. *Electrochimica Acta*. 2015; 165:330-337.

\*\*\*\*\*